CARBON 62 (2013) 240–247

Available at www.sciencedirect.com

SciVerse ScienceDirect

journal homepage: www.elsevier.com/locate/carbon

Wear of carbon fiber reinforced carbon matrix composites: Study of abrasive, oxidative wear and influence of humidity

Soydan Ozcan [a,*], *Peter Filip* [b,c]

[a] *Materials Science and Technology Division, Oak Ridge National Laboratory, Oak Ridge, TN, USA*
[b] *Center for Advanced Friction Studies, Southern Illinois University, Carbondale, IL, USA*
[c] *Department of Mechanical Engineering and Energy Processes, Southern Illinois University, Carbondale, IL, USA*

ARTICLE INFO

Article history:
Received 17 January 2013
Accepted 15 May 2013
Available online 13 June 2013

ABSTRACT

The wear of C/C composites has been studied using a subscale aircraft brake dynamometer linked with a mass spectrometer. A disc-on-disc configuration allowed for simulation of various aircraft landing energy conditions (12.5%, 25%, 50%, and 100% of normal landing energy of a Boeing 737 aircraft) performed at 50% and 90% relative humidity levels. The microstructure of composite brakes was altered by applying three different heat treatment temperatures: 1800, 2100, and 2400 °C, respectively. A mass spectrometer linked to an environmental chamber of the subscale dynamometer was utilized to measure the in situ CO_2 release during the wear tests. The relationships between microstructure, hardness of individual components of composites and wear performance at varied conditions are presented. Carbons obtained at higher heat treatment temperatures are most vulnerable to abrasive wear, while the less ordered carbons, typical for samples heat treated at lower temperatures, showed significant amount of oxidative wear. Oxidative wear was related to excessive heating of materials. Optimization of wear behavior of C/C composite is only possible by understanding the mechanisms of the microstructural changes of materials, corresponding mechanical properties and the nature of wear under various environmental conditions.

Published by Elsevier Ltd.

1. Introduction

Friction and wear characteristics of carbon fiber reinforced carbon (C/C) composite brakes are affected by a number of factors including service environment (temperature, adsorption and desorption of water vapor, oxygen partial pressure, and contaminants), fiber reinforcement and architecture, matrix type, friction process parameters (normal load, sliding speed, and energy), and composite surface features (roughness, grooves) and formed friction layer [1,2]. Friction behavior of carbon has been studied since the 1920s. Bragg first discovered the crystal structure of graphite by X-ray diffraction in 1928 [3], and he introduced a theory on the lubrication characteristics of graphite based on the crystal structure. This theory involved the easy shearing of adjacent graphene sheets due to weak bonding between them resulting in lubrication and low friction behavior. The large spacing between the graphene sheets was assumed to be the reason for the weak bonding between them. Even though this theory was questioned, it was widely accepted. Subsequently, Savage found that the lack of water vapor in the environment leads to high wear and high coefficient of friction in graphite [4–6]. This is also known as "dusting regime". It was reported that dry air, H_2, N_2, and inert gases are unable to avoid the

* *Corresponding author:* Fax: +1 865 241 2158.
E-mail address: ozcans@ornl.gov (S. Ozcan).
0008-6223/$ - see front matter Published by Elsevier Ltd.
http://dx.doi.org/10.1016/j.carbon.2013.05.061

dusting regimes [5,7–9]. According to Pardee and Campbell, O_2 and CO_2 prevent dusting regime above the partial pressure at which these gasses are present in ordinary air [7,10]. Savage stated that organic vapors are much more effective than water vapor for avoiding dusting regimes [11]. Furthermore, Rowe suggested that water vapor and oxygen could penetrate into the graphene sheets and reduce the shear strength [9,12]. They suggested these vapors could weaken the π-bonding between graphene sheets by "stress etching" during cleavage [9,13,14]. In contrast, Bryant et al. observed, interlamellar energy is much higher when oxygen and water vapor are available than with the lack of them under a vacuum atmosphere [13,14]. Moreover, measurement of lattice parameters of graphite by X-ray diffraction showed that d-spacing does not increase by the vapor intercalation [15]. However, Arnell and Teer indicated that there are considerable limitations of the d-spacing measurements by X-ray diffraction to define the possibility of the weakening of interplanar bonding near the graphite surface [15]. In addition, investigation of the surface using X-ray diffraction from a synchrotron source by Yen et al. showed that, there is no change in the d-spacing of graphite near the surface as the outgassed graphite sample is exposed to the ambient and humid air environments [16].

According to Deacon and Goodman, low friction behavior of graphite is due to the chemisorption of vapor molecules and the formation of dangling bonds at the edge of graphite crystals. They suggested that the reacted vapor forms various oxygenated surface groups which result in reduction of the bonding force between crystallites [17]. Yen's study on four different carbon materials showed that graphite, non-graphitic carbon and C/C composites exhibit similar tendencies in the friction process when the dry nitrogen and dry air environments are altered [18,19]. This study supports the view that a higher coefficient of friction is associated with a dry nitrogen environment as opposed to the high oxygen partial pressure (i.e., air) environment. The reported studies showed that adsorption effect of condensing vapor, which causes lubrication, is responsible for low friction behavior. Conversely, desorption of vapor during friction is responsible for the dusting regime. On the other hand, Bragg's lattice-shear model [3] maintains its attraction as an additional explanation for the lubrication of graphite. Nevertheless, Gouider et al. used a pin-on-disc tester equipped with a mass spectrometer and directly observed the consumption of O_2 and release of CO_2 when the dusting regime and a transition from low to high friction occurred [20]. They also stated that oxidation was sustained as long as the coefficient of friction and wear remained high [20,21]. It is suggested that water vapor oxidizes the carbon with hydrogen release as a product of the reaction [20]. It is now generally accepted that the mechanical, thermal, chemical properties of composites; characteristics of the formed friction layer on the contact surface; and adsorption/desorption of gases and vapors are all of essential concern in relation to friction performance of C/C composites. The objective of this study is to generate new knowledge and to understand the fundamental principles of controlling the friction and wear performance by establishing the aforementioned relationships between friction performance, microstructure and properties.

Table 1 – Sample notifications and corresponding final heat treatment temperatures.

Heat treatment temperature (°C)	Sample notification
1800	CC-D18
2100	CC-D21
2400	CC-D24

2. Experimental

2.1. Materials

Three directional needled felt PAN-based carbon fiber reinforced carbon matrix commercial composites were kindly provided by Honeywell Aircraft Landing System™ in forms of discs with diameter of 600 mm and thickness 25 mm. Carbon fiber preforms were densified using chemical vapor infiltration (CVI) technique. As received CVI densified samples were heat-treated using a graphitization furnace (model: TP-4X10-G-G-D64A-A-27, Centorr Associates Inc). Heat treatment was performed in an argon protective atmosphere (~0.5 bar) for 1 h at temperatures of 1800, 2100 and 2400 °C, and named as CC-D18, CC-D21, and CC-D24, respectively (Table 1). The bulk density of samples was measured after heat treatment using helium pycnometry method. Densities are measured as 1.97 g/cm^3 (CC-D18), 2.06 g/cm^3 (CC-D21), and 2.11 g/cm^3 (CC-D24). The open porosity level was 8.77% before heat treatment using a mineral spirit method [2]. The microstructure and mechanical properties of bulk samples used in this study reported in authors' previous publication [22].

2.2. Friction and wear tests

The friction and wear tests were performed using a Link Engineering sub-scale aircraft brake dynamometer (Model 2076, Plymouth, MI, USA) on C/C composite discs scaled down in accordance with the energy/mass ratio. The nominal outer and inner diameters of the ring specimens were 92.25 mm (3.75″) and 69.85 mm (2.75″), respectively. The schematic diagram of the computer, controlled subscale, aircraft dynamometer equipped with environmental chamber is shown in Fig. 1.

A mass spectrometer (Hewlett Packard 5970) was coupled with the subscale dynamometer system and the gaseous products released during braking were continuously monitored along with atmospheric Argon (Ar), which served as a convenient reference standard for CO_2 analysis. Normalized results from the MS (CO_2/Ar ratio) were correlated to wear of the C/C composite measured as mass loss.

The friction and wear tests simulated different scenarios with 12.5, 25, 50 and 100% of a Boeing 737 normal landing energy (NLE). The relative humidity level (50% or 90%) was maintained with a humidity control system within ±2% of the desired value. The subscale aircraft brake dynamometer was operated in constant torque mode, the normal force varied in response to the current coefficient of friction to achieve the desired torque set point (2.041 kgf m). For the period of the braking process, a number of parameters such as stop

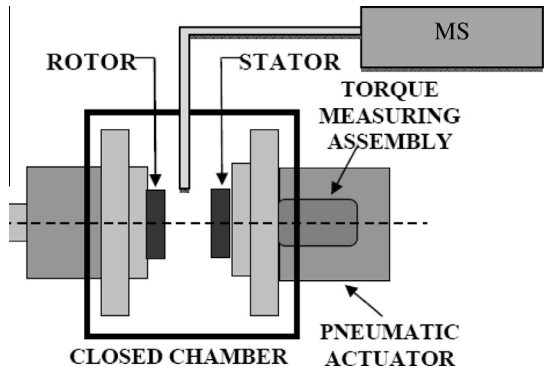

Fig. 1 – Schematic diagram of subscale aircraft dynamometer set-up used in research.

time: (7–34 s), contact pressure (0.08–0.35 MPa) and speed (202.8 km/h) were controlled. A sequence of three "taxi stops" performed at 4.5% NLE followed by one "landing stop" was repeated 50 times for each energy condition (a total of 200 braking events). The initial temperature of each test stop was set at $T_0 = 50$ °C (120°F) and the applied normal force ramp rate dF/dt was set at the value of 1780 N/s (400 lb/s). The coefficient of friction, temperature, torque, deceleration rate and normal force were measured in real time. The testing conditions [2] are given in Table 2.Wear was determined as the mass loss after each series of 200 stops for individual energy conditions applied:

$$W(\text{wt.}\%) = \frac{M_{\text{pre}} - M_{\text{post}}}{M_{\text{initial}}} \times 100 \quad (1)$$

where M_{initial} is the initial mass of tested C/C composite (always identical), M_{pre} is the mass of sample before testing, M_{post} is the mass of sample after testing. A high precision digital scale (Metler-Toledo, AB135-S) with an accuracy of ±0.01 mg was used for the mass measurements.

2.3. *Nanoindentation*

The C/C composite specimens with dimensions approximately 15 ×15 ×15 mm were randomly cut from different discs for nanoindentation measurements, mounted into an epoxy resin, ground and then polished using diamond polishing slurries with a grain size ranging from 6 to 0.25 μm. The polishing was completed with a 0.05 μm grain size alumina suspension. Nanohardness of C/C composites was measured on polished surfaces at room temperature using a Nano Indenter® XP system (MTS Nanoinstruments, Knoxville, TN) with a Berkovich-type diamond tip. (AccuTip™ with the radius of curvature about 40–50 nm). Before each test, the system was calibrated using a fused silica. The continuous stiffness mode was used for the tests. Thirty randomly selected different fiber and thirty CVI carbon matrix locations were indented for each sample.

2.4. *Microscopy and surface topography*

Scanning electron micrographs of the fractured surfaces of C/C composites were obtained using Hitachi S570, Tokyo, Japan Scanning Electron Microscopy (SEM).

2.5. *Topographical characterization of friction surface*

Topography of the contact surfaces after friction tests was measured using a Mahr Perthometer PRK skidless-stylus-type profilometer with a diamond tip. The typical tip radius is 5 μm and maximum vertical resolution is 7 nm. A diamond tip dragged a single trace across a surface to generate a trace that is representative of the actual surface. The scanned nominal friction surface was an 8 by 8 mm area and included 256 traces. Each trace included 22,400 data points.

3. Results and discussions

3.1. *Effect of humidity, surface temperature and energy on wear*

Fig. 2 shows the wear as detected at different humidity levels and energy conditions for all three C/C composite sample heat-treated at different temperatures. Obviously, wear of C/C composites depends on humidity, energy and carbon microstructure (type of heat treatment). The lowest wear was detected for the C/C composites heat treated at 2100 °C and tested at 90% relative humidity. The impact of humidity is quite large at lower landing energy conditions (12.5% and 25% NLE), when the temperature does not reach the critical values necessary for complete evaporation of adsorbed species. A considerably higher wear was detected for samples tested at 12.5% and 25% NLE and 50% RH (solid lines in Fig. 2) when compared to wear of samples tested at 90% RH and identical energies (dashed lines in Fig. 2). This is typical and due to lack of formation of friction layer on rubbing surface [1]. Friction layer does not form or is discontinuous at low landing energy simulations (12.5% and 25% NLE). It has been observed that after the formation of friction layer, required higher energy landing conditions, wear decreases

Table 2 – Testing parameters at different energy levels during friction tests.

	Taxi (4.5% NLE)	12.5% NLE	25% NLE	50% NLE	100% NLE
Energy (J)	5786.35	16100.36	32200.72	64401.44	128802.871
Stop time (s)	7.2	34	34	34	34
Inertia (kg m^2)	1.796	1.796	1.796	1.796	1.796
Rot. speed (rpm)	766.59	1278.39	1807.92	2556.78	3615.83
Rot. speed (rpm)	80.28	133.87	189.32	267.75	378.65
Torque (N/m)	20.03	7.07	10	14.15	20.01

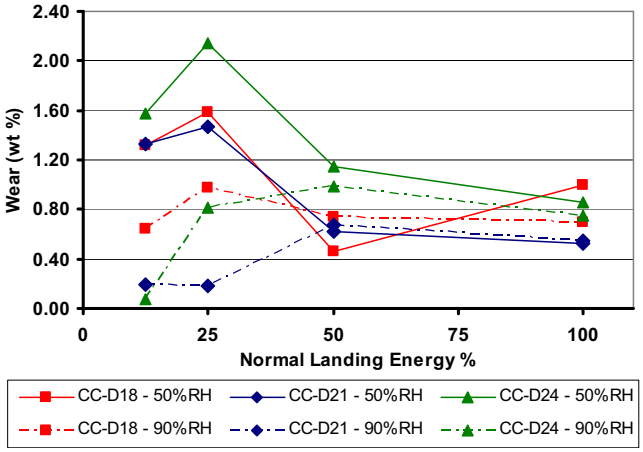

Fig. 2 – Wear of C/C samples subjected to different HTTs, tested in subscale aircraft dynamometer at various energy and humidity conditions.

considerably [1]. When tested above 50% NLE, these drastic differences due to humidity impact are mitigated and the microstructure of carbon seems to play the most important role when wear performance is concerned.

It has been suggested by various researchers that the role of water vapor adsorption and desorption play significant role in friction and wear of carbonaceous materials [23–26]. Reduced water vapor in the environment leads to high wear and high coefficient of friction in graphite and other carbon forms [23]. Moisture on the surface acts as a lubricating agent; wear of material stays low until the moisture has evaporated from the surface. Once the surface temperature reaches the necessary level to evaporate the moisture, the first transition of the coefficient friction is observed [23]. The corresponding transition leads to the dusting regime [7,8,11,24]. The friction test results of the investigated composites (Fig. 2) showed that moisture significantly influenced the wear at low energy braking simulations (12,5% and 25% NLE) for all three materials. While all composites exhibited the highest wear at 50% RH and low energy conditions (12.5% and 25% NLE), they displayed the lowest wear at 90% RH and low energy conditions. This is an evidence of the strong effect of adsorbed water on wear at low energy landing simulations. In a high humidity environment (90% RH), the friction surface temperature remained low and the adsorbed water vapor did not evaporate from the friction surface, typically no transition of the coefficient of friction is observed as reported earlier [23] and the wear remained low (Fig. 2). On the other hand, humidity does not have as large of an impact on a wear rate at 50% and 100% NLE. The temperature on the friction surface reaches high values rapidly, and the water vapor suddenly evaporates from the friction surfaces. Clearly the variation of the humidity level in 100% NLE simulations did not appear to have a notable effect on the wear of CC-D21 and CC-D24 but did for CC-D18. The high wear rate of CC-D18 is due to the extensive oxidation at 50% RH, as evidenced from CO_2 measurements during tests (presented later). It seems that high humidity in the environment reduces the excessive wear of CC-D18 as compared to 50% RH testing environment. This shows that the presence of high humidity in the environment has lubricating effects, keeps the surface cooler and delayed and reduced the oxidation.

3.2. *Abrasive wear and nanohardness*

Abrasive wear is usually considered as primary wear mechanism and occurs when a surface containing hard particles, slides on a softer surface and ploughs a series of grooves [25,26]. The nanohardness results of CC-D samples are plotted in Fig. 3. Based on measurement orientation, hardness of the fiber varies considerably, while the values detected for the CVI matrix are similar for the parallel and normal directions with respect to the fiber axis. The nanohardness of the CVI matrix decreased from 1.86 to 0.99 GPa with increasing heat treatment temperature. Considerably softer microstructures are more prone to abrasive wear. Conversely, the hardness of PAN based C-fibers increased from 2.69 GPa detected for samples heat treated at 1800 °C to 3.65 GPa measured for samples subjected to 2400 °C HTT when measured on polished cross sections parallel with longitudinal axis of C-fiber. While the hardness of fiber and matrix is similar for NHT sample, the large detected difference between fiber and matrix, observed after applied heat treatment will considerably influence the wear process. Hard C-fiber particles generated during the friction process lead to a significant abrasive wear of the soft CVI carbon. The wear of CC-D24 was higher (Fig. 3) compared to other samples and the abrasive wear mechanism obviously dominates the wear of CC-D24 samples.

However, as shown in Fig. 4, the increase of the final heat treatment temperature of the studied C/C composite samples also introduced more cracks into the C/C composite structure. This is a result of thermal stresses generated due to different thermal expansions of C-fibers and CVI matrices [27]. The thermally induced cracks not only compromise the microstructural integrity of the samples but also contribute to an increase in oxidative wear of the samples heat treated at 2400 °C. It is also known that interfacial shear strength between fiber and matrix drastically decreases with increasing heat treatment temperature [28,29] and it is obvious from

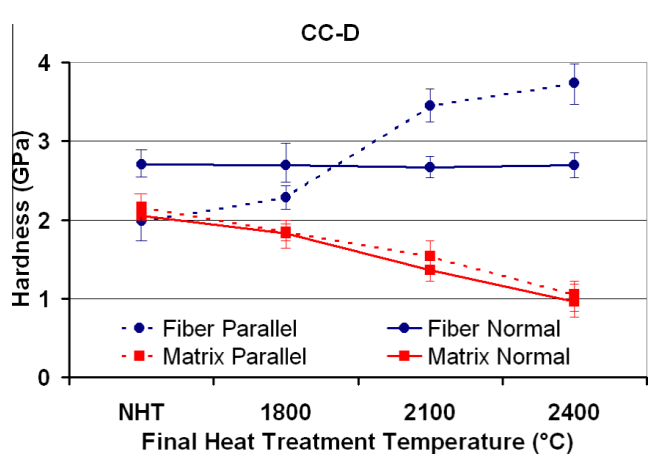

Fig. 3 – Measured hardness of C-fiber and CVI-matrix detected in CC-D composites subjected to different heat treatment temperatures. The error bars represent 2 standard deviations. NHT: not heat-treated samples.

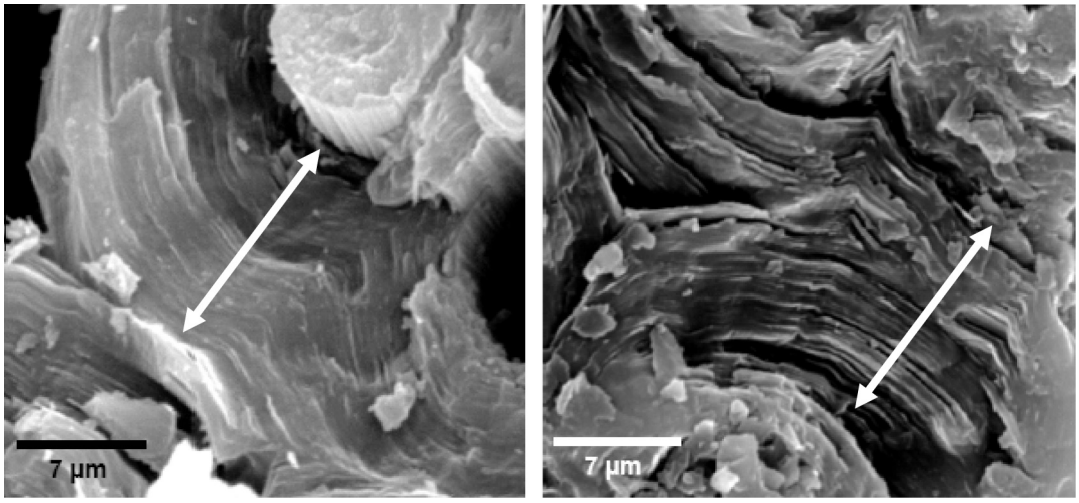

Fig. 4 – SEM micrographs of fractured surfaces showing the typical CVI matrices in CC-D18 (a) and CC-D24 (b). CC-D18 has few cracks; however, numerous cracks are clearly seen in CCD-24 due to graphitization of matrix. Arrows show the transverse section of pyrocarbon matrices.

Fig. 4 that numerous thermal cracks effectively allow for increased transport of oxidative species into structure [30,31]. The thermally activated reorientation of the graphitic planes during HTT at higher temperatures also leads to formation of extensive shrinkage cracks in CC-D24 matrix. All newly formed cracks provide entrance paths for transport of oxidative species into the C/C composites. Thereby, the high heat treatment temperature increases the oxidative capacity and oxidative wear of CC-D24 even at low energy landing simulations.

Surface waviness values of friction surfaces observed after different aircraft landing simulations performed at 50% RH conditions are shown in Fig. 5. Both the surface waviness (Fig. 5) of friction surfaces increased with increased heat treatment temperature of the C/C composites and the applied energy during the landing simulations. The grooves seen on the friction surfaces are generated by abrasive action of harder particles in the composites and are formed more extensively when the hardness differences between C-fiber and CVI matrix increase as discussed above. Interestingly, the presence of conforming grooves results in an increasing dynamic satiability of brake discs and leads to reduction of vibration and noise [32].

3.3. *In situ mass spectroscopy*

Mass spectroscopy (MS) allowed to measure the released CO_2 amounts during simulated braking at different conditions and to correlate those measurements with wear results. The data illustrated in Fig. 6 represent an example of normalized CO_2/Ar quantities obtained for the material heat treated at 2400 °C tested at 50% RH and 50% NLE.

The amounts of released CO_2 are proportionally related to oxidative wear. As easily seen from Fig 6, the simulated landings are typified by similar and relatively large amounts of CO_2 release, while taxi stops are characterized by a very low oxidation. Obviously, wear of C/C composites detected at low energy simulations (Fig. 3) is mostly abrasive in nature.

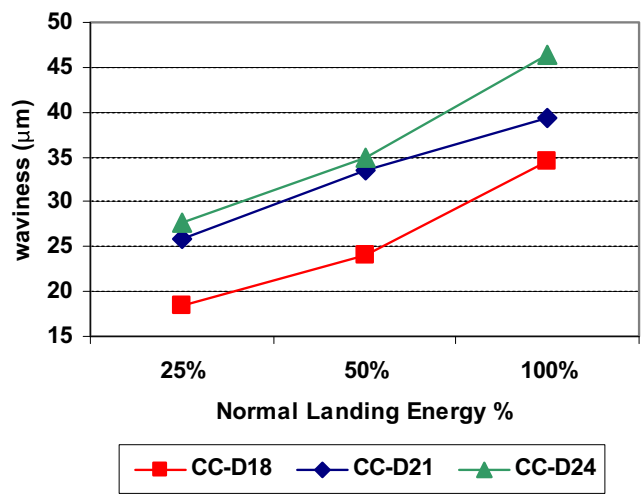

Fig. 5 – Surface waviness data after the friction test performed at 50% relative humidity conditions and 25%, 50%, and 100% NLE simulations.

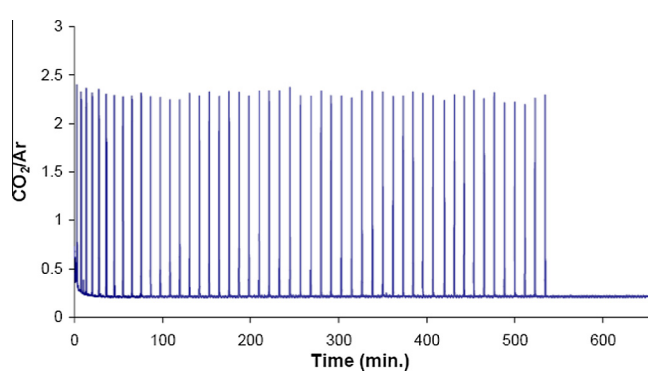

Fig. 6 – Representative mass spectroscopy data normalized to atmospheric Ar for CC-D24 material obtained for simulated 50% landing energy conditions performed at 50% relative humidity environment.

As easily seen from Fig. 7, the total amount of CO_2 released during dynamometer braking simulations varied depending on the final heat treatment temperature and the simulated landing conditions. The MS results indicate that the released CO_2 amount was almost identical at all simulated landing energy conditions for CC-D24 (Fig. 7). For CC-D21, however, the amount of released CO_2 almost doubled at 100% NLE relative to the low energy landing conditions. CO_2 release was also significantly higher at high-energy testing condition for CC-D18 samples. In this material, the CO_2 release increased four times from 0.34 detected at 50% NLE simulations to 1.38 measured for 100% NLE, as seen in Fig. 7. This can be attributed to the relatively poor thermal conductivity of CC-D18 through the thickness due to the presence of less ordered carbon [22,33,34]. CC-D18 reaches the highest friction surface temperature during braking among the investigated composites, which significantly accelerates the oxidation reaction rate of the carbon [35]. Interestingly, at 25% and 50% NLE simulations, the amount of released CO_2 detected for CC-D24 with the highest thermal conductivity is almost twice that of the other two tested composites. Even if the high temperature heat treatment has improved the crystallinity of carbon and thus the thermal conductivity and resistance to oxidation, the formation of thermal cracks during the high temperature heat treatment leads to an increase of the oxidation level.

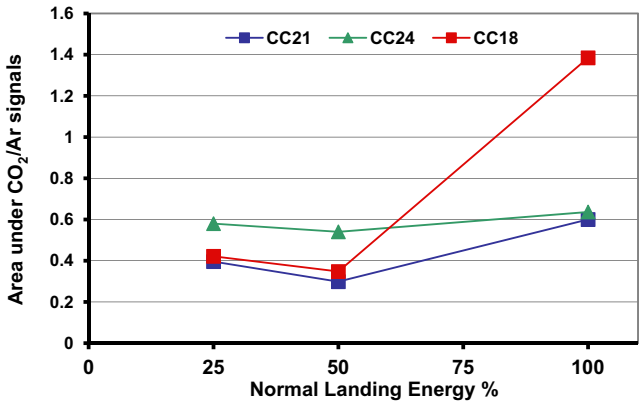

Fig. 7 – The cumulative CO_2/Ar ratio (total area under the peaks) for heat-treated materials detected at 50% RH and different dynamometer NLE conditions.

The CC-D21 sample exhibited the lowest CO_2 release at all energy conditions indicating the highest oxidation resistance during friction tests [31,35]. Past research on oxidation of the

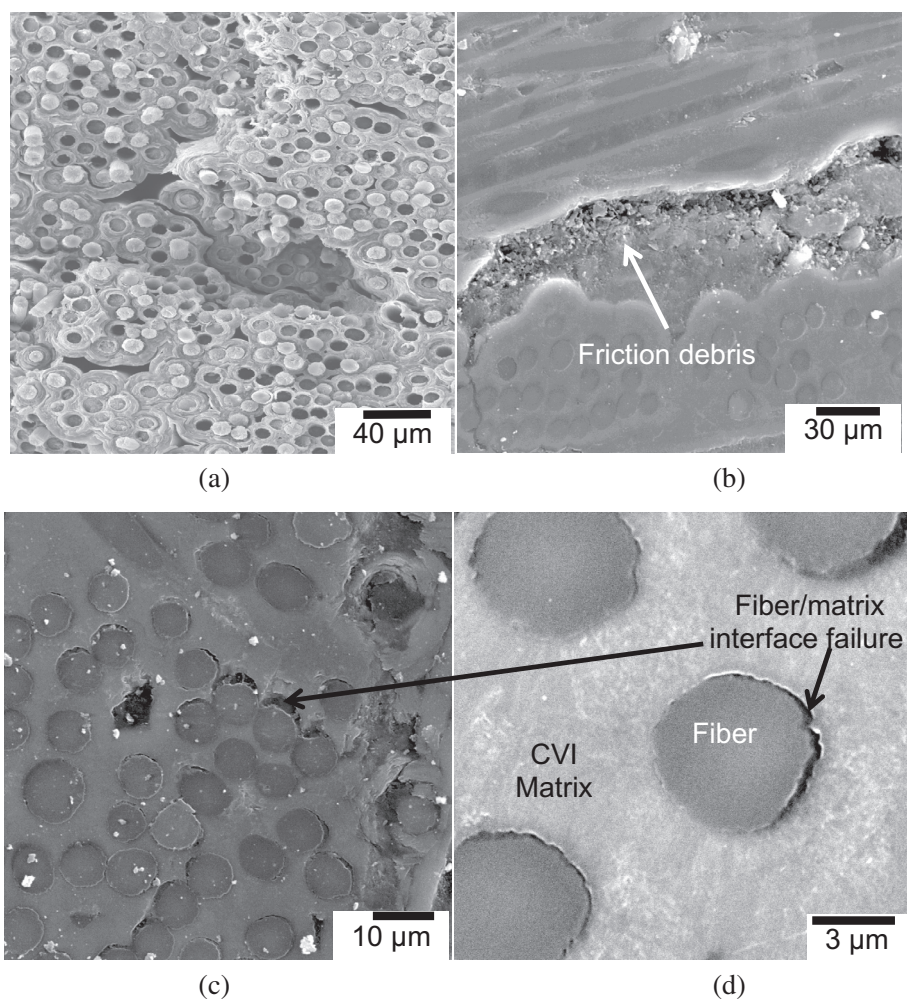

Fig. 8 – Fractured surface of CC-D24 composite (a), friction surface of CC-D24 after 100% NLE braking simulations at 50% RH (b–d).

investigated C/C composites by thermogravimetric analysis, showed that 2100 °C heat treatment optimizes oxidation resistance [35]. The sample subjected to heat treatment at 1800 °C is particularly sensitive to oxidation when tested at 100% NLE simulations.

The wear debris captured between two rubbing surfaces transforms into a friction layer and forms a new type of material different from the bulk carbon types (Fig. 8). The friction layer consists of crushed and/or sintered friction layers. Friction layer on the rubbing surface forms by complex mechanochemical interactions and breakdown of crystallites with an applied high energy. The formed friction layer on the contact surface significantly influences wear performance of C/C composites and needs to be studied in conjunction with frictional performance of C/C composites. It is also seen that the fracture tip deviates at the fiber/matrix interface (Fig. 8c and d) after friction process, which is an indication of noteworthy role of fiber matrix interface bonding in braking process.

4. Conclusions

Subscale dynamometer simulations revealed that, among the three applied heat treatment temperatures, 2100 °C was found to be the most favorable heat treatment temperature for achieving minimum wear and acceptable frictional properties of the investigated C/C composites. When the difference between hardness of C-fiber and CVI matrix, respectively, is large due to structure development in the applied heat treatment cycle, a high abrasive wear and formation of waviness was detected. A high oxidative wear was detected in structures with a less organized carbon (samples subjected to a lower HTT) and numerous cracks formed as a result of thermal stresses generated during heat treatment. Shrinkage cracks and thermal stress cracks were observed in samples exposed to a HTT of 2100 °C and more extensive cracking was seen in the samples heat treated at 2400 °C. These cracks primarily follow the fiber/matrix interface. The interface failures have been observed after braking experiments and expected to be playing a role on wear performance of C/C composites. Mass spectroscopy results revealed dominating oxidative wear in samples subjected to 1800 °C HTT (less ordered carbon). While CC-D18 exhibited a promising performance at low energy conditions, mass spectroscopy reveals its severe oxidation during 100% NLE braking simulations.

In accord with the previously published data, it was confirmed that humidity has a significant impact on friction and wear of C/C composites. This study demonstrated clearly that the adsorbed moisture inhibits the high wear particularly seen at the low energy braking simulations. Since the high friction surface temperatures led to a rapid evaporation of moisture from the friction surfaces, adsorbed moisture does not inhibit wear at high energy landing scenarios. SEM studies showed that wear debris accumulated in pores and friction layer always developed on the rubbing surfaces. It is highly possible that the microstructure of the formed friction layer is markedly influencing the friction and wear properties of C/C composite materials. The formation and influence of friction layer requires detailed further investigation.

Acknowledgments

This research was sponsored by the National Science Foundation (Grant EEC 3369523372), State of Illinois and a consortium of 11 industrial partners of the Center for Advanced Friction Studies. Authors also would like to acknowledge the team members at Center for Advanced Friction Studies for their help on experiments.

REFERENCES

[1] Ozcan S. Microstructure–property–performance relationships of carbon-fiber-reinforced carbon composite friction materials. PHD Dissertation, Southern Illinois University. 2008.
[2] Krkoska M. Effect of relative humidity and kinetic energy on frictional performance of C/C composite materials (disc-on-disc configuration). Carbondale: Southern Illinois University; 2007.
[3] Bragg SWH. An introduction to crystal analysis. London: G. Bell and Sons, Ltd; 1928.
[4] Savage RH. Carbon brush contact films. Gen Electr Rev 1945;48:13–20.
[5] Savage RH. Graphite lubrication. J Appl Phys 1948;19:1–10.
[6] Savage RH, Schaefer DL. Vapor lubrication of graphite sliding contacts. J Appl Phys 1956;27:136–8.
[7] Pardee RP. Moisture dependence of silver-graphite brushes in air, nitrogen, helium, and carbon dioxide. IEEE Trans Power App Syst 1967;86(5):616–25.
[8] Ramadanoff D, Glass SW. High-altitude brush problem. Trans AIEE 1944;63:825–9.
[9] Lancaster JK, Pritchard JR. The influence of environment and pressure on the transition to dusting wear of graphite. J Phys D 1981;14(4):747.
[10] Campbell WE, Kozak R. Studies in boundary lubrication III. The wear of carbon brushes in dry atmospheres, Trans. ASME 1948;70:491–7.
[11] Savage RH. Physically and chemically adsorbed films in the lubrication of graphite sliding contacts. Ann NY Acad Sci 1951;53(4):862–9.
[12] Rowe GW. Some observations on the frictional behavior of boron nitride and of graphite. Wear 1960;3(4):274–85.
[13] Bryant PJ, Gutshall PL, Taylor LH. A study of mechanisms of graphite friction and wear (lamellar solid lubrication based on hypothesis which correlates interlayer binding energy and frictional phenomena). Wear 1964;7:118–26.
[14] Bryant PJ, Lavik M, Salomon G, Hinrichs CH. Mechanisms of solid friction. Am J Phys 1965;33(7):593.
[15] Arnell RD, Teer DG. Lattice parameters of graphite in relation to friction and wear. Nature 1968;218:1155–6.
[16] Yen BK, Schwickert BE, Toney ME. Orgin of low-friction behavior in graphite investigated by surface x-ray diffraction. Appl Phys Lett 2004;84(23):4702–4.
[17] Deacon RF, Goodman JF. Lubrication by lamellar solids. Proc R Soc London, Ser A 1958;243(1235):464–82.
[18] Yen BK. Influence of water vapor and oxygen on the tribology of carbon materials with sp^2 valence configuration. Wear 1996;192(1–2):208–15.
[19] Yen BK, Ishihara T. An investigation of friction and wear mechanisms of carbon–carbon composites in nitrogen and air at elevated temperatures. Carbon 1996;34(4):489–98.
[20] Gouider M, Berthier Y, Jacquemard P, Rousseau B, Bonnamy S, Estrade-Szwarckopf H. Mass spectrometry during C/C composite friction: carbon oxidation associated with high friction coefficient and high wear rate. Wear 2004;256(11–12):1082–7.

[21] Kasem H, Bonnamy S, Rousseau B, Estrade-Szwarckopf H, Berthier Y, Jacquemard P. Interdependence between wear process, size of detached particles and CO_2 production during carbon/carbon composite friction. Wear 2007;263(7–12):1220–9.
[22] Ozcan S, Tezcan J, Filip P. Microstructure and elastic properties of individual components of C/C composites. Carbon 2009;47(15):3403–14.
[23] Ozcan S, Krkoska M, Filip P. Frictional performance and local properties of C/C composites. Ceram Eng Sci Proc 2005;26(8):127–38.
[24] Lancaster JK. Transitions in the friction and wear of carbons and graphites sliding against themselves. Tribol Trans 1975;18(3):187–201.
[25] Blau PJ. Friction and wear transitions of materials. Park Ridge, NJ (USA): Noyes Publications; 1989.
[26] Blau PJ. Friction science and technology. New York: Marcel Dekker; 1996.
[27] Ozcan S, Filip P. Influence of final heat treatment on microstructure and thermal properties of C/C composites. ASME-GSRIC Proceedings. Tulsa, OK; 2007.
[28] Gurung B. Mesurement of the fiber/matrix interfacial strength of carbon carbon composites by nanoindentation. Carbondale, IL: Southern Illinois University; 2007.
[29] Tezcan J, Ozcan S, Gurung B, Filip P. Measurement and analytical validation of interfacial bond strength of PAN-fiber-reinforced carbon matrix composites. J Mater Sci 2008;43(5):1612–8.
[30] Peszynska-Bialczyk K, Krkoska M, Pawliczek A, Filip P, Anderson K. Study of "adsorption/desorption" phenomena on friction debris of aircraft brakes. Developments in Advanced Ceramics and Composites: Ceramic Engineering and Science Proceedings. 2005:157–166.
[31] Peszynska-Bialczyk K, Anderson KB, Szymanski T, Krkoska M, Filip P. Thermal analysis of bulk carbon–carbon composite and friction products derived from it during simulated aircraft braking. Carbon 2007;45(3):524–30.
[32] Farhang K, Ozcan S, Filip P. The effect of wear groove on vibration and noise of aircraft brakes: theoretical and experimental evidence. SAE Int J Passenger Cars-Mech Syst 2009;1(1):1223–9.
[33] Ozcan S. Microstructure and related properties of carbon/carbon composite aircraft brakes. Carbondale: Southern Illinois University; 2004.
[34] Ozcan S, Woldemicheal M, Iqbal S, Filip P. Microstructure and thermal properties of 2 and 3 directionals C/C composites. Ceram Eng Sci Proc 2007;27(2):233–44.
[35] Peszynska-Bialczyk K, Thomas S, Filip P. Activation energy of oxidation processes of carbon/carbon composites after applying different final heat treatment temperatures. Semi Annual Report; Center for Advanced Friction Studies-SIUC. 2006;11(1):1–12.